Domain Decomposition and Mixed Finite Elements for the Neutron Diffusion Equation

Françoise Coulomb*†

Abstract. Among the classical methods used for solving the neutron diffusion equation, an iterative power method combined with a finite element method allows an efficient numerical treatment. A domain decomposition method seems well suited to the structure of a parallel computer. As the domains and data are often almost symmetrical, the mixed elements method yields well uncoupled systems. Some decompositions along the axes of symmetry are considered and numerically treated on two examples of reactors.

1. **Introduction.** The steady state formulation of the multigroup diffusion equation is the following (4,5):

$$- \mathrm{Div}(D_g(r)\nabla\Phi_g(r)) + \Sigma_g^t(r)\ \Phi_g(r) = \sum_{g'=1}^{G} \left[\frac{1}{\lambda}\chi_g \nu\Sigma_{g'}^f(r) + \Sigma_{g'g}^t(r)\right]\Phi_{g'}(r) \tag{1}$$

for g = 1 ... G

with: Φ_g = neutron flux in group g
D_g = diffusion coefficient in group g
Σ_g^t = total removal cross section in group g
Σ_g^f = macroscopic fission cross section for group g
$\Sigma_{gg'}^t$ = macroscopic scattering cross section from group g to group g'

* Service d'Etudes de Réacteurs et de Mathématiques Appliquées, Centre d'Etudes Nucléaires de Saclay, 91191 Gif-sur-Yvette Cedex, France.
† Laboratoire d'Analyse Numérique, Université Pierre et Marie Curie, 75005 Paris, France.

χ_g = fission spectrum for prompt neutrons
ν = average number of neutrons produced per fission
λ = effective multiplication factor
G = total number of energy groups
r = spacial dependence.

The boundary conditions are of Neumann-Dirichlet type.

This is generally solved by an iterative power method (4,5) combined with a finite element method ; it is reminded that the power method for solving an equation of the form: $M\Phi = \frac{\nu}{\lambda} F\Phi$, can be written:

$$\begin{cases} \psi^{(n+1)} = \nu\, M^{-1}\, F\Phi^{(n)} \\ \lambda^{(n+1)} = \dfrac{(1,\ F\,\psi^{(n+1)})}{(1,\ F\Phi^{(n)})} \\ \Phi^{(n+1)} = \dfrac{1}{\lambda^{(n+1)}}\,\psi^{(n+1)} \end{cases} \qquad \text{(outer)iteration } n+1$$

A parallel computer with four processors on-line has already been built for demonstration [1,2] ; it runs now with a Lagrange finite elements method ; the inner iterations technique is presently a parallel version of the block S.O.R. method (more precisely, an odd-even block S.O.R. method) ; the domain is partitioned into lines in 2D (planes in 3D), and each processor treats a set of contiguous lines (or planes).

As the matrices obtained through mixed elements methods are not positive definite, few results ensure the convergence of block Jacobi and block S.O.R. methods. In the case of complete symmetry, with an appropriate choice of the initial vector, the convergence of the block Jacobi and block S.O.R. methods holds in 1 iteration ; that is why, when the data are almost symmetrical, a domain decomposition along the axes of symmetry is used to get a parallel preconditionner ; by doing so and by choosing an appropriate initial vector for the iterations, a fast convergence of the previous iterative methods is expected. In practice, there are four axes (planes) of symmetry, so the domain is naturally splitted into eight parts ; in a new parallel computer project there will be eight processors ; we intend to assign a subdomain to each processor, this explains why we concentrate on the block Jacobi method.

The contents of the paper are as follows: in section 2, the mixed-dual variational formulation of the problem and its approximations are reminded ; in section 3, some decompositions are described and justified ; in section 4, they are tested on two examples of reactors and the numerical results are interpreted.

2. The mixed-dual method (6,7).

2.1. The variational formulation. Each iteration of the power method yields problems of the following form:

$$- \mathrm{Div}(D\nabla u) + \Sigma u = S \qquad \text{in } \Omega \tag{2}$$

with Dirichlet-Neumann boundary conditions: $\begin{cases} u = 0 & \text{on } \Gamma_0 \\ D\dfrac{\partial u}{\partial n} = 0 & \text{on } \Gamma_1 \end{cases}$

Ω being a bounded domain of $\mathbb{R}^n$ (n = 2,3) representing the core and $\partial\Omega = \Gamma_0 \cup \Gamma_1$, $\Gamma_0 \cap \Gamma_1 = \phi$.

In the mixed-dual formulation, the flux u and the current "$\vec{p} = D\vec{\nabla}u$" appear as independant variables ; the variational formulation is the following:

$$\left| \begin{array}{l} \text{Find } (\vec{p},u)\in H_{0,\Gamma_1}(\text{div},\Omega) \times L^2(\Omega) \text{ so that:} \\ \int_\Omega \frac{1}{D}\,\vec{p}.\vec{q} + \text{div}\,\vec{q}\,u = 0 \qquad \forall\vec{q}\in H_{0,\Gamma_1}(\text{div},\Omega) \\ \int_\Omega -\text{div}\,\vec{p}\,v + \Sigma uv = \int_\Omega Sv \qquad \forall v\in L^2(\Omega) \end{array} \right. \tag{3}$$

where

$$\left| \begin{array}{l} H_{0\Gamma_1}(\text{div},\Omega) = \{\vec{q}\in H(\text{div},\Omega) \;/\; \langle\gamma_1(\vec{q}),v\rangle = 0 \quad \forall v\in H^1_{0,\Gamma_0}(\Omega)\} \\ \gamma_1(\vec{q}) = \text{normal derivative of } \vec{q} \\ H^1_{0,\Gamma_0}(\Omega) = \{v\in H^1(\Omega) \;/\; \gamma_0(v) = 0 \quad \text{on } \Gamma_0\} \\ \gamma_0(v) = \text{trace of } v \end{array} \right.$$

It is well known that under the assumptions:

$$\left| \begin{array}{l} D,\Sigma\in L^\infty(\Omega) \\ 0 < \nu \leqslant D(x) \text{ and } 0 \leqslant \Sigma(x) \quad \text{a.e. in } \Omega \\ f\in L^2(\Omega) \\ \partial\Omega \text{ "regular", meas}(\Gamma_0) > 0 \end{array} \right. \tag{4}$$

problem (3) has a unique solution ($\vec{p} = D\vec{\nabla}u,u$), where u is the solution of the classical primal problem:

$$\left| \begin{array}{l} \text{Find } u\in H^1_{0,\Gamma_0}(\Omega) \text{ so that:} \\ \int_\Omega D\,\vec{\nabla}u.\vec{\nabla}v + \Sigma uv = \int_\Omega Sv \qquad \forall v\in H^1_{0,\Gamma_0}(\Omega) \end{array} \right. \tag{5}$$

2.2. Approximation of the solution. Equation (3) is approximated by a finite element technique ; the approximation spaces are:

$$\left| \begin{array}{l} Q_h = \left\{\vec{q}_h\in H_{0,\Gamma_1}(\text{div},\Omega)/\vec{q}_h\in Q_K \qquad \forall K\in T_h\right\} \\ V_h = \left\{v_h\in L^2(\Omega) \qquad /v_h\in P_K \qquad \forall K\in T_h\right\} \end{array} \right.$$

T_h being a triangulation, P_K and Q_K polynomial spaces.

Let us suppose that Ω is a union of rectangles or parallelepiped rectangles, and T_h a regular family of triangulations constituted of (parallelepiped) rectangles. Let T_h be one of the triangulations. For all given integers k, ℓ, m, let us denote $P_{k,\ell}$ and $P_{k,\ell,m}$ the following spaces:

$$\left|\begin{array}{l} P_{k,\ell} = \{P\in\mathbb{R}[X,Y] \;/\; \deg_x P \leqslant k \quad \deg_y P \leqslant \ell\} \\ P_{k,\ell,m} = \{P\in\mathbb{R}[X,Y,Z] \;/\; \deg_x P \leqslant k \quad \deg_y P \leqslant \ell \; \deg_z P \leqslant m\} \end{array}\right.$$

In the method of Raviart and Thomas, for each K:

$$\left|\begin{array}{lll} Q_K = P_{k+1,k} \times P_{k,k+1} & P_K = P_{k,k} & \text{in 2D} \\ Q_K = P_{k+1,k,k} \times P_{k,k+1,k} \times P_{k,k,k+1} & P_K = P_{k,k,k} & \text{in 3D} \end{array}\right.$$

k being a given integer ; the approximations of u and $\vec{p}$ are of order k+1. A modified method gives: $\begin{cases} Q_K = P_{\ell+1,0} \times P_{0,\ell+1} \\ P_K = P_{\ell,0} + P_{0,\ell} \end{cases}$; this method is of order 1 whatever integer ℓ may be.

2.3. Description of a mixed-dual element of order 1 in 2D: MXOL5 (3). The finite element basis can be represented in terms of unknowns as shown in fig. 1.

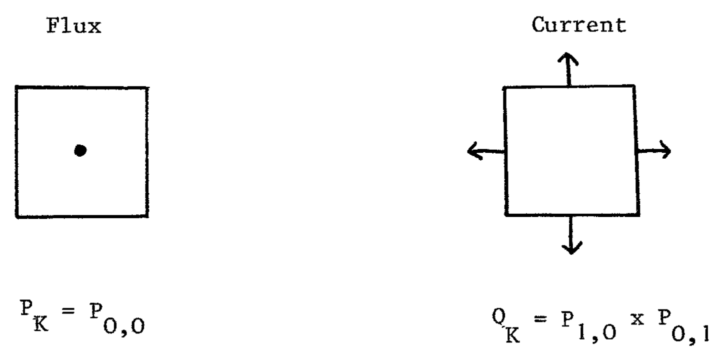

FIG. 1: *Mixed element of order 1 MXOL5. There is one internal node for the flux, and the current unknowns are the constant values of* $\vec{p}_h \cdot \vec{n}$ on *each edge.*

This element MXOL5 is so-called because on each rectangle the approximation of u is constant, the approximation of $\vec{p}$ is linear, and there are 5 unknowns.

3. Domain decomposition. For the sake of simplicity, we restrict ourselves to the 2D case ; in 3D, there are analogous results.

In practice, we are often in the presence of a domain of the form indicated in fig. 2, which has four axes of symmetry (in 3D the domains have four planes of symmetry) and the data are almost symmetrically distributed ; here, only the horizontal and vertical axes are considered.

Decompositions along the axes of symmetry are the purpose of this study.

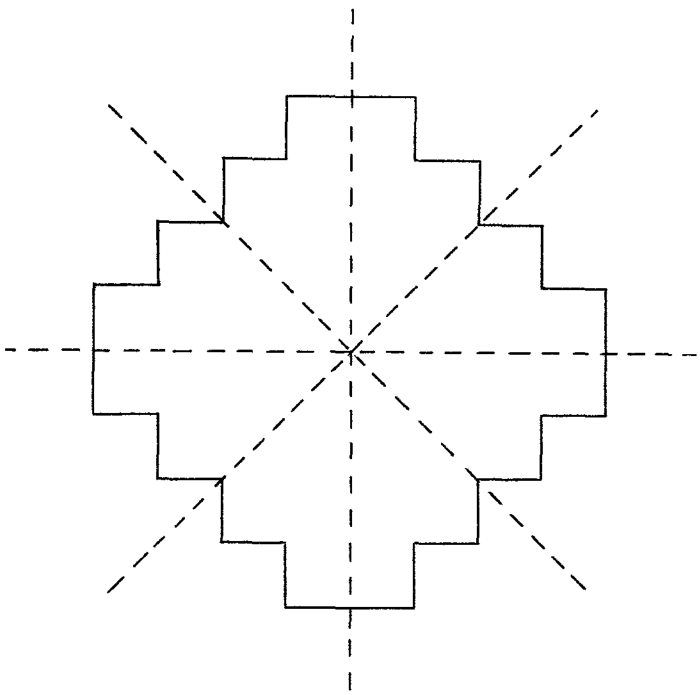

FIG. 2: *General form of the domain. The axes of symmetry are indicated in dotted-lines.*

In the sequel, it is supposed that:

(h1) Ω has an axis of symmetry Δ, and, Γ_0 and Γ_1 are symmetric with respect to Δ.

For each point $y \in \mathbb{R}^2$, $\tilde{y}$ denotes the mirror image of y with respect to Δ, and for each vector $\vec{z}$, $\hat{\vec{z}}$ denotes the mirror image of $\vec{z}$ with respect to the direction of Δ : $\vec{\Delta}$.

3.1. **Symmetry of the solution.** Let us suppose that the data D, Σ and S are symmetric with respect to Δ (condition (h2)). Then the solution satisfies:

$$\begin{cases} \vec{p}(\tilde{x}) = \hat{\vec{p}}(x) \\ u(\tilde{x}) = u(x) \end{cases}$$

The same result holds for the approximate solution, provided that:

$$(h3) \quad \begin{vmatrix} w_h \in V_h \iff W_h \in V_h \\ \vec{q}_h \in Q_h \iff \vec{Q}_h \in Q_h \end{vmatrix}$$

where: $W_h(x) = w_h(\tilde{x})$ and $\vec{Q}_h(x) = \vec{q}_h(\tilde{x})$.
Under the following assumptions:

(h4) the edges of the rectangles composing Ω are parallel to the axes of coordinates.
(h5) Δ is the x-axis or the y-axis.
(h6) T_h is symmetric with respect to Δ (see fig. 3).
(h7) the finite element of reference is of the R. and T. type.

property (h3) holds.

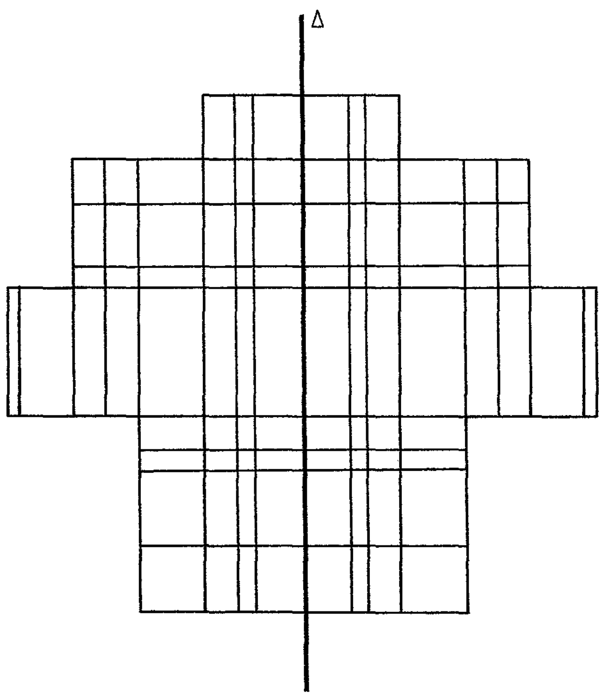

FIG. 3: *Symmetry of the triangulation* T_h

3.2. **The block Jacobi method.** The domain will be decomposed along the axes of symmetry.

Assume that (h4) and (h5') are verified, (h5') being the condition: Δ is the y-axis. Ω is splitted into two parts:

$$\Omega_1 = \left\{z = \begin{pmatrix} x \\ y \end{pmatrix} \in \Omega \;/\; x < 0\right\}$$
$$\Omega_2 = \left\{z = \begin{pmatrix} x \\ y \end{pmatrix} \in \Omega \;/\; x > 0\right\}$$

The interface $\left\{z = \begin{pmatrix} x \\ y \end{pmatrix} \in \bar{\Omega} / x = 0\right\}$ is denoted Γ_3 ($\Gamma_3 \subset \Delta$). We have the choice of considering Γ_3 separately or as part of one of the subdomains.

The nodes are numbered in the following order: first those of $\bar{\Omega}_1 \backslash \Gamma_3$ then those of $\bar{\Omega}_2 \backslash \Gamma_3$, and to end those of Γ_3.

Γ_3 is supposed to be composed of edges of rectangles $K \in T_h$ (condition (h8)) (see fig. 4).

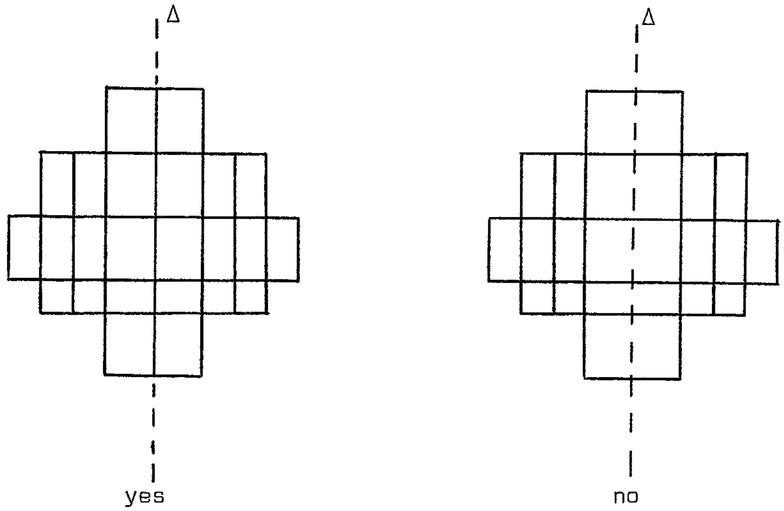

FIG. 4: *The domain is splitted into two parts with an interface composed of edges of rectangles* $K \in T_h$ *on the left figure ; the figure on the right shows a bad splitting.*

The matrix of the linear system has the following form:

$$A = \begin{pmatrix} A_{11} & 0 & A_{13} \\ 0 & A_{22} & A_{23} \\ {}^tA_{13} & {}^tA_{23} & A_{33} \end{pmatrix} \tag{6}$$

and we have to solve $A \begin{pmatrix} x_1 \\ x_2 \\ x_3 \end{pmatrix} = \begin{pmatrix} B_1 \\ B_2 \\ B_3 \end{pmatrix} = B$, with $B_3 = 0$, for all the nodes on Γ_3 are current nodes.

A_{11} is the matrix of the approximate problem corresponding to the equation:
$$\begin{cases} -\operatorname{div}(D\nabla u) + \Sigma u = S & \text{in } \Omega_1 \; ; \\ u = 0 & \text{on } \Gamma_0 \cap \partial\Omega_1 \\ D \dfrac{\partial u}{\partial n} = 0 & \text{on } (\Gamma_1 \cap \partial\Omega_1) \cup \Gamma_3 \end{cases}$$

Meas $(\Gamma_0) > 0$ and Γ_0 is symmetrix with respect to Δ (hypothesis h1), so meas $(\Gamma_0 \cap \partial\Omega_1) > 0$; then A_{11} is invertible. For the same reason A_{22} is invertible. As A_{33} is the matrix of the positive definite bilinear form: $(\vec{p},\vec{q}) \to \int_\Omega \frac{1}{D}\, \vec{p}.\vec{q}$ on a subspace of Q_h, A_{33} is invertible. So, the block Jacobi method can be considered.

Let (h9) be the condition:

> For the element of reference $\hat{K}$, the unknowns are symmetrically distributed with respect to its vertical axis of symmetry.

Proposition: Under the assumptions (h2), (h6), (H7) and (h9), and if the initial vector $X^{(0)}$ satisfies:

(h10)
$$\begin{cases} X^{(0)}(i) = -X^{0}(j) & \text{if i and j are gradient nodes corresponding to the x-component of } p_h \text{, and are symmetric with respect to } \Delta. \\ X^{(0)}(i) = X^{0}(j) & \text{in the other case if i and j are symmetric with respect to } \Delta. \end{cases}$$

then the block Jacobi method converges in 1 iteration.

proof: it is not restrictive to suppose that the numbering of the nodes is done as follows:

. in domain 1, the first nodes to be numbered are those corresponding to the flux ; for the current nodes, we first number the nodes corresponding to the x-component of p_h, then those corresponding to the y-component,

. the nodes of domain 2 are numbered symmetrically with respect to the axis of symmetry.

Then A has the following form:

$$A = \begin{pmatrix} A^F_{11} & A^{FX}_{11} & A^{FY}_{11} & 0 & 0 & 0 & A^F_{13} \\ {}^tA^{FX}_{11} & A^X_{11} & 0 & 0 & 0 & 0 & A^X_{13} \\ {}^tA^{FY}_{11} & 0 & A^Y_{11} & 0 & 0 & 0 & 0 \\ 0 & 0 & 0 & A^F_{11} & -A^{FX}_{11} & A^{FY}_{11} & -A^F_{13} \\ 0 & 0 & 0 & -{}^tA^{FX}_{11} & A^X_{11} & 0 & A^X_{13} \\ 0 & 0 & 0 & {}^tA^{FY}_{11} & 0 & A^Y_{11} & 0 \\ {}^tA^F_{13} & {}^tA^X_{13} & 0 & -{}^tA^F_{13} & {}^tA^X_{13} & 0 & A_{33} \end{pmatrix} = \begin{pmatrix} A_{11} & 0 & A_{13} \\ 0 & A_{22} & A_{23} \\ {}^tA_{13} & {}^tA_{23} & A_{33} \end{pmatrix}$$

We have also:

$$B = \begin{pmatrix} B^F_1 \\ B^X_1 \\ B^Y_1 \\ B^F_2 \\ B^X_2 \\ B^Y_2 \\ B_3 \end{pmatrix} = \begin{pmatrix} B^F_1 \\ 0 \\ 0 \\ B^F_1 \\ 0 \\ 0 \\ 0 \end{pmatrix} \qquad X^{(0)} = \begin{pmatrix} X^{(0)}_{1F} \\ X^{(0)}_{1X} \\ X^{(0)}_{1Y} \\ X^{(0)}_{1F} \\ -X^{(0)}_{1X} \\ X^{(0)}_{1Y} \\ 0 \end{pmatrix} = \begin{pmatrix} X^{(0)}_1 \\ X^{(0)}_2 \\ 0 \end{pmatrix}$$

At the first iteration, we have:

$$\begin{cases} A_{11}\, X^{(1)}_1 = B_1 - A_{13}\, X^{(0)}_3 = B_1 \\ A_{22}\, X^{(1)}_2 = B_2 - A_{23}\, X^{(0)}_3 = B_2 \end{cases}$$

but, $X_3 = 0$ and so $\begin{cases} A_{11}\, X_1 = B_1 \\ A_{22}\, X_2 = B_2 \end{cases}$; then $\begin{cases} X^{(1)}_1 = X_1 \\ X^{(1)}_2 = X_2 \end{cases}$.

$$A_{33}\, X_3^{(1)} = 0 - {}^tA_{13}\, X_1^{(0)} - {}^tA_{23}\, X_2^{(0)}$$

$$A_{33}\, X_3^{(1)} = 0 - \left({}^tA_{13}^F \quad {}^tA_{13}^X \quad 0\right)\begin{pmatrix} X_{1F}^{(0)} \\ X_{1X}^{(0)} \\ X_{1Y}^{(0)} \end{pmatrix} + \left(- A_{13}^F \quad {}^tA_{13}^X \quad 0\right)\begin{pmatrix} X_{1F}^{(0)} \\ -X_{1X}^{(0)} \\ X_{1Y}^{(0)} \end{pmatrix}$$

$$A_{33}X_3^{(1)} = - {}^tA_{13}^F\, X_{1F}^{(0)} - {}^tA_{13}^X\, X_{1X}^{(0)} + A_{13}^F\, X_{1F}^{(0)} + {}^tA_{13}^X\, X_{1X}^{(0)} = 0$$

So $X_3^{(1)} = 0 = X_3$, and $X^{(1)} = X$.

We notice that the Gauss-Seidel method converges in one iteration with the only assumption that $X_3^{(0)} = 0$.

If Γ_3 is considered as part of one of the subdomains, we have no more this property of convergence in one iteration ; the hypothesis should be ${}^tA_{23}\left(X_2^{(0)} - X_2\right) = 0$ for example and that cannot be satisfied if some of the components of X_2 are not known.

There is an analogous result if there are two axes of symmetry and if the interface is considered as a fith domain.

The previous result explains why, if Ω has axes of symmetry, we decompose it along these axes ; when the data are almost symmetrical, we hope to have a fast convergence with the decomposition of dissection type (the interface is considered as a separate domain).

On a parallel computer, we shall assign a domain to each processor, and (eventually) the interface to the host processor.

4. Numerical tests. We have restricted ourselves to the 2D case and have carried out tests on two examples of reactor, choosing the mixed element MXOL5 ; some decompositions of the core have been considered. The numerical results led us to a study of the block Jacobi method on a simple example.

4.1. Description of the two reactors

4.1.1. The 2D IAEA Benchmark. It corresponds to a median plane of a 3D problem representing an idealized model of a Pressurized Water Reactor. This reactor contains four homogeneous regions (see fig. 5):

(1) a region of high enrichment
(2) a region of slight enrichment
(3) a region where the control absorbants have been mixed with the fuel
(4) a light water reflector.

4.1.2. The 2D Tihange. This problem represents a reactor at the begining of the second cycle. The heterogeneity of the core induces a checkerboard effect on the power distribution. It is a good representation of the different real reactor types ; its geometry is represented in fig. 6.

4.2. Description of the tests. The tests have been carried out with the mixed element MXOL5, on a CRAY-XMP.

In the two examples, Ω is symmetric with respect to the coordinates axes ; in the Benchmark case, the data are symmetric, but they are not in the Tihange case.

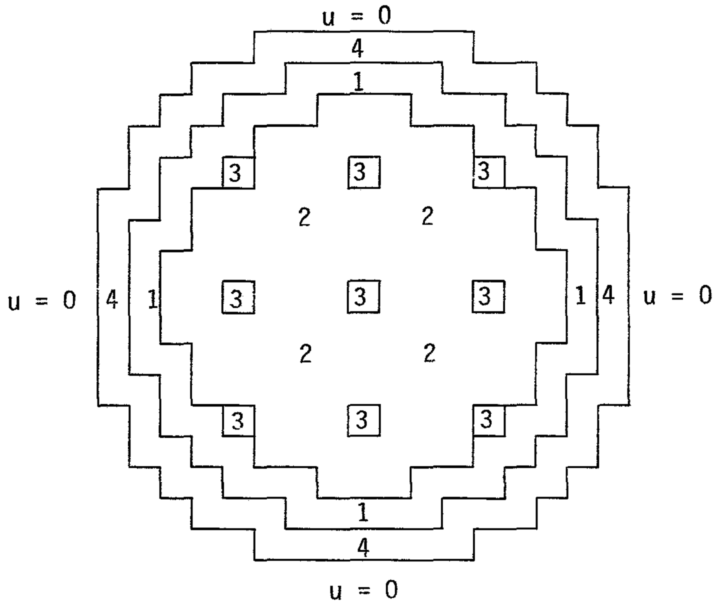

Size of an assembly : 20 cm

FIG. 5: *The 2D IAEA Benchmark*

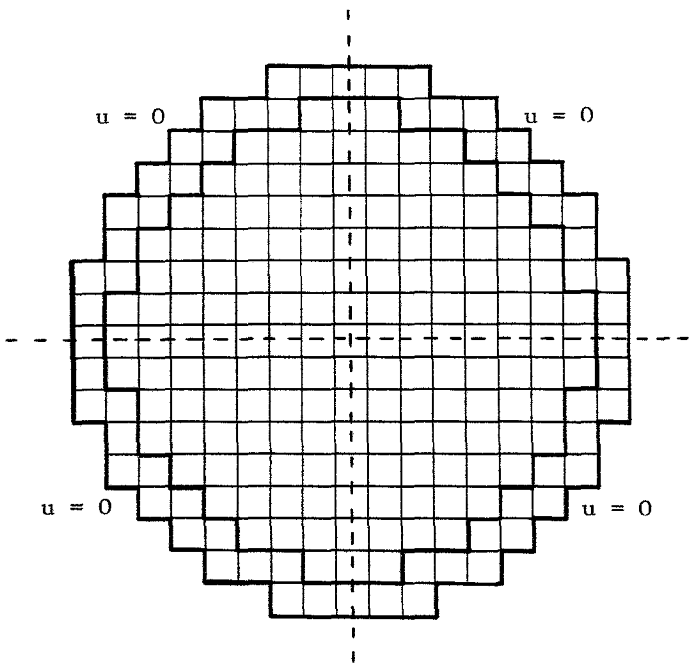

Size of an assembly : 21,5313 cm

FIG.6: *The 2D Tihange. Geometry: representation of the complete core.*

The meshes that are used are the following:
. 1 block per assembly, except for the assemblies on the axes of symmetry which are divided by these ones ;

. 4 blocks per assembly ; we note: "2×2" (see fig. 7).

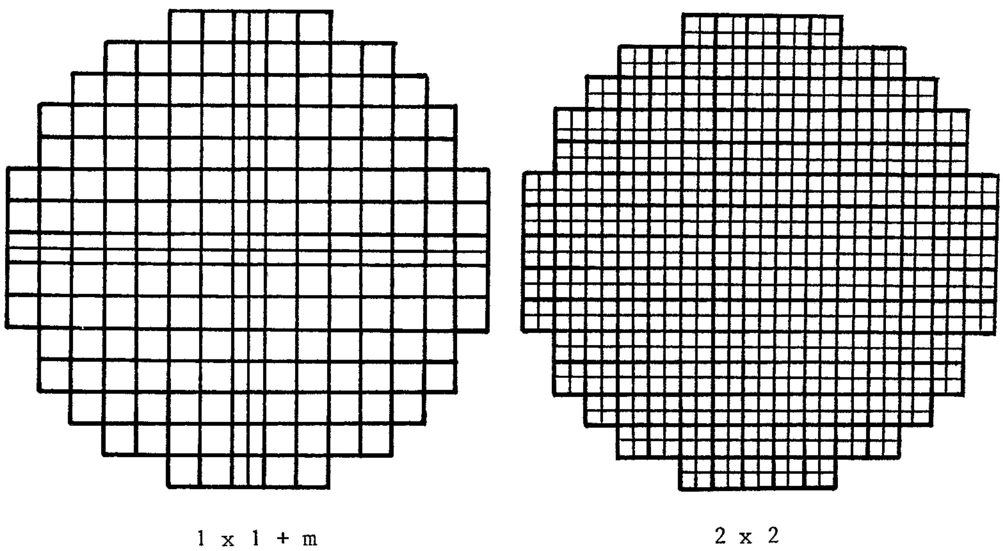

FIG. 7: *The two meshes: "1×1+m" and "2×2" for the reactor Tihange.*

Ω is split up either into two or into four subdomains ; we have the choice of considering the interface separately or as part of the subdomains ; that gives four decompositions named "2B", "2B+I", "4B" and "4B+I" (see fig. 8).

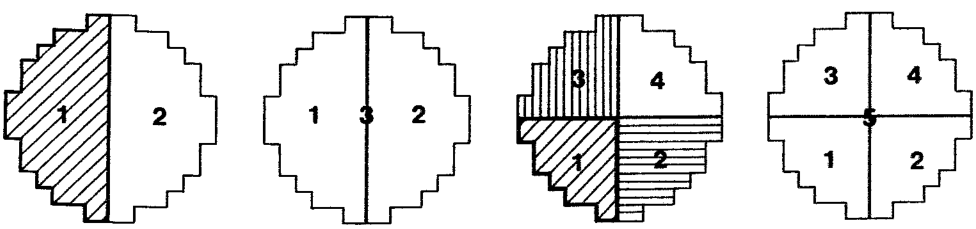

FIG.8: *The four decompositions of the domain.*

The stopping criteria are:

$$\left\| \frac{u_n}{\|u_n\|} - \frac{u_{n-1}}{\|u_{n-1}\|} \right\| \leqslant \text{epsf} \qquad \text{for the flux}$$

$$\frac{|\lambda_n - \lambda_{n-1}|}{|\lambda_n|} \leqslant \text{epsv} \qquad \text{for the current}$$

For the first test (Benchmark), we know that on the coordinates axes we have: $\vec{p}_h.\vec{n} = 0$ theoretically ; it was decided that $\vec{p}_h.\vec{n}$ should be numerically considered equal to zero if $|\vec{p}.\vec{n}| < 10^{-5}$.

4.3. Numerical results. Some numerical results are shown in Tables I.1, I.2, I.3 for the Benchmark, in Tables II.1 and II.2 for the Tihange.

TYPI indicates the solving method for the inner iterations: J stands for Jacobi, G.S. for Gauss-Seidel (S.O.R.) and C for a direct solving.

2 inner iterations are performed for each outer iteration, and the process is stopped after 150 iterations if the convergence is not yet obtained.

Table I.1

epsf = 5.10^{-4} epsv = 10^{-4}

Mesh	TYPI	Eigenvalue	Memory place (words)	Iter. time (c)	nb. iter.	Decomp.	Remarks
1 × 1 + m	C	1,03320059	67444	35	20	/	┼ 0
2 × 2	C	1,03336754	244200	89	15	/	┼ 0
1 × 1 + m	J	1,03318790	39266	146	51	2B	├→ 10^{-4} ⊥↑ 0
1 × 1 + m	G.S.	1,03320060	39266	58	20	2B	┼ 0
2 × 2	J	1,03332931	173374	479	49	2B	├→ 4.10^{-5} ⊥↑ 0
1 × 1 + m	J	1,03320060	39154	57	20	2B + I	├→ $1,2.10^{-5}$ ⊥↑ 0
1 × 1 + m	G.S.	1,03320060	39154	61	20	2B + I	┼ 0
2 × 2	J	1,03336754	172718	143	15	2B + I	┼ 0
1 × 1 + m	J	1,03319254	38500	210	73	4B	├→ $7,6.10^{-4}$ ⊥↑ $7,6.10^{-4}$
1 × 1 + m	G.S.	1,03317949	38500	73	24	4B	├→ $2,5.10^{-4}$ ⊥↑ $7,6.10^{-4}$
2 × 2	J	1,03333493	170288	274	69	4B	├→ $4,5.10^{-5}$ ⊥↑ $7,6.10^{-4}$
1 × 1 + m	J	0,53648906	38260	442	150	4B + I	maxi. preci.: (iter.18) flux: 8.10^{-4} λ: $1,6.10^{-5}$

In the last column ('Remarks'), we indicate especially the order of magnitude of $|\vec{p}_h.\vec{n}|$ on the interface:

$\mapsto$ r indicates that $|\vec{p}_h.\vec{n}|$ is at a maximum of r on the vertical interface.

It is to note that, as we are only testing the method, the storage has not been optimized: the matrices have been stockpiled in a "profil" way ; we intend to stock the diagonal blocks of the matrices in this way, and the off-diagonal matrices by a 'Morse' storage.

For the initialization, the current was taken equal to 0 and the flux equal to 1.

Table I.2

epsf = 10^{-6} epsv = 10^{-6}

Mesh	TYPI	Eigenvalue	Memory place (words)	Iter time (c)	nb. iter	Decomp.	Remarks
1 × 1 + m	J	0,79205594	39154	437	150	2B + I	$\underline{\uparrow}$ 0 $\mapsto$ 1 maxi. preci.: (around iter.19) flux: $3{,}5.10^{-4}$ eigenvalue: 2.10^{-6}
1 × 1 + m	J	1,03325707	39266	420	150	2B	$\underline{\uparrow}$ 0 $\mapsto$ 2.10^{-5} after iter. 145, the prec. is of: 10^{-8} for λ 10^{-6} for the flux ($> 10^{-6}$)

Table I.3

epsf = 5.10^{-3} epsv = 10^{-4}

Mesh	TYPI	Eigenvalue	Memory place (words)	Iter time (c)	nb. iter	Decomp.	Remarks
1 × 1 + m	J	1,03202216	39154	35	12	2B + I	$+$ 0
1 × 1 + m	J	1,03198796	39266	62	22	2B	$\mapsto$ 9.10^{-4} $\underline{\uparrow}$ 0
1 × 1 + m	J	1,03202216	38260	35	12	4B + I	$+$ 0
1 × 1 + m	J	1,03226591	38500	86	30	4B	$\mapsto$ 5.10^{-3} $\underline{\uparrow}$ 0

Table II.1

epsf = 10^{-5} epsv = 10^{-5}

Mesh	TYPI	Eigenvalue	Memory place (words)	Iter time (c)	nb. iter	Decomp.	Remarks
2 × 2	C	1,00331257	220469	210	36	/	
2 × 2	J	1,00331263	159578	631	66	2B	if epsf=10^{-4}, conv. is reached at iter 36
2 × 2	J	0,92635364	158864	1432	150	2B + I	maxi. preci.: flux: 8.10^{-5} λ: 5.10^{-7} between iter 47 and 60, $\lambda \approx 1,003315$
2 × 2	J	1,00331274	156422	1424	150	4B	if epsf=10^{-4}, conv. is reached at iter 51
2 × 2	J	0,53890438	155334	1445	150	4B + I	max. prec.: flux: $1,4.10^{-3}$ λ: 4.10^{-6} between iter 15 and 18 $1,003314 \leqslant \lambda \leqslant 1,003320$

Table II.2

epsf = 2.10^{-3} epsv = 10^{-5}

Mesh	TYPI	Eigenvalue	Memory place (words)	Iter time (c)	nb. iter	Decomp.	Remarks
2 × 2	C	1,00332450	220469	58	10	/	
2 × 2	J	1,00330566	159578	124	13	2B	$\frac{124}{2} = 62 \approx 58$
2 × 2	J	1,00332981	158864	95	10	2B + I	$\frac{95}{2} = 47,5 < 58$
2 × 2	J	1,00331549	156422	247	19	4B	$\frac{247}{4} = 61,75 \approx 58$
2 × 2	J	1,00332985	155334	116	12	4B + I	$\frac{116}{4} = 29 \ll 58$

4.4. Commentaries and interpretations

4.4.1. Benchmark test. The basic mesh for the interpretation is the mesh "1×1+m".

We first stated: epsf = 5.10^{-4} and epsv = 10^{-4}, as it is generally done in our code for the Benchmark. Firstly, we see that as stated mathematically, in the two cases of direct solving, there are properties of symmetry for the flux and the current, and $\vec{p}.\vec{n}$ is *nil* on the axes of symmetry. We notice that for the decomposition 4B + I, there are some problems ; that is why, we wanted to see what happened in the case 2B + I for a greater requested precision, and also for all the cases for a lower precision.

For a requested precision of 5.10^{-3} for the flux and 10^{-4} for the eigenvalue, the decompositions for which the interface is separated (2B + I, 4B + I) are by far the fastest ones, and they give a best approximation of $\vec{p}.\vec{n}$ on the interface. That still holds for a precision of 5.10^{-4} and 10^{-4} for the case 2B + I.

For the decompositions 2B + I and 4B + I, we note that for each outer iteration (at least for the first ones), the result is the same for the first and second iterations of the block Jacobi method ; this confirms the mathematical result that tells that the Jacobi method converges in one iteration with an appropriate initialization. In these two cases, it is noticed that after having reached a certain precision during several iterations:

$$\begin{cases} 5.10^{-4} \text{ and } 2.10^{-6} & \text{for 2B + I} \\ 5.10^{-3} \text{ and } 5.10^{-5} & \text{for 4B + I} \end{cases}$$

the results deteriorate, and become quite different from the solution. If we look more precisely, we notice that the property of converging in one iteration for the Jacobi method holds exactly only during $\begin{cases}\text{19 iterations for 2B + I} \\ \text{14 iterations for 4B + I}\end{cases}$, and the error at the second iteration increases, the process being more accentuated for the case 4B + I ; so, if at that point the requested precision is not reached, problems may appear. That can be partly explained by the fact that numerical results are not exact results ; here, after a certain number of iterations, we may loose slightly properties of symmetry and so, at the beginning of the Jacobi iterations, the starting vector has no more the property for the convergence in one iteration.

Increasing the number of inner iterations doesn't provide better results for the cases 2B and 4B, and may occur difficulties for the two others, because of the process discussed about above.

In the case of a requested precision of 5.10^{-4} for the flux and 10^{-4} for the eigenvalue, we note that the Gauss-Seidel method is faster than the Jacobi method and gives a better approximation of $\vec{p}_h.\vec{n}$ on the axes of symmetry.

4.4.2. Tihange test. The previous phenomena are amplified. With the mesh "2×2" the decompositions with a separated interface can only reach a precision of:

$$\begin{cases} 10^{-4} \text{ for the flux, } 10^{-6} \text{ for the eigenvalue} & \text{in the case 2B + I} \\ 2.10^{-3} \text{ for the flux, } 4.10^{-6} \text{ for the eigenvalue} & \text{in the case 4B + I} \end{cases}$$

4.5. Third test. The previous results led to a study of the block Jacobi method for a very simple case:

. Ω is a square, $\Gamma_0 = \partial\Omega$

. the triangulation is obtained by a splitting into four parts

. the functions D, Σ and S are set constant

. the mixed element is still MXOL5.

The unknowns are numbered as indicated on fig. 9.

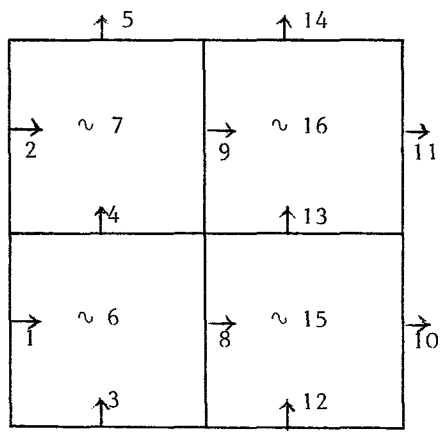

FIG.9: *Numbering of the nodes.*

The decomposition that are considered are the same as before:

- 2B : domain 1 ⟷ nodes: 1,2,3,4,5,6,7,8,9
  domain 2 ⟷ nodes: 10,11,12,13,14,15,16
- 2B + I: domain 1 ⟷ nodes: 1,2,3,4,5,6,7
  domain 2 ⟷ nodes: 10,11,12,13,14,15,16
  domain 3 ⟷ nodes: 8,9
- 4B : domain 1 ⟷ nodes: 1,8,3,4,6
  domain 2 ⟷ nodes: 10,12,13,15
  domain 3 ⟷ nodes: 2,9,5,7
  domain 4 ⟷ nodes: 11,14,16
- 4B + I: domain 1 ⟷ nodes: 1,3,6
  domain 2 ⟷ nodes: 10,12,15
  domain 3 ⟷ nodes: 2,5,7
  domain 4 ⟷ nodes: 11,14,16
  domain 5 ⟷ nodes: 8,9,4,13

The matrix of the linear system is the following, with $\alpha = \frac{1}{6D}$:

$$A = \begin{bmatrix}
2\alpha & & & & & -1 & & \alpha & & & & & & & & \\
& 2\alpha & & & & & -1 & & \alpha & & & & & & & \\
& & 2\alpha & \alpha & & -1 & & & & & & & & & & \\
& & \alpha & 4\alpha & \alpha & 1 & -1 & & & & & & & & & \\
& & & \alpha & 2\alpha & & 1 & & & & & & & & & \\
-1 & & -1 & 1 & & -\Sigma & & 1 & & & & & & & & \\
& -1 & & -1 & 1 & & -\Sigma & & 1 & & & & & & & \\
\alpha & & & & & 1 & & 4\alpha & & \alpha & & & & & -1 & \\
& \alpha & & & & & 1 & & 4\alpha & & \alpha & & & & & -1 \\
& & & & & & & \alpha & & 2\alpha & & & & & 1 & \\
& & & & & & & & \alpha & & 2\alpha & & & & & 1 \\
& & & & & & & & & & & 2\alpha & \alpha & & -1 & \\
& & & & & & & & & & & \alpha & 4\alpha & \alpha & 1 & -1 \\
& & & & & & & & & & & & \alpha & 2\alpha & & 1 \\
& & & & & & & -1 & & 1 & & -1 & 1 & & -\Sigma & \\
& & & & & & & & -1 & & 1 & & -1 & 1 & & -1
\end{bmatrix}$$

The interest concerned particularly the decomposition 4B + I, because in the previous examples, it was with this decomposition that some problems arised.

We took: $\begin{cases} D = \frac{1}{600}, \frac{1}{6}, \frac{100}{6} \\ \Sigma = 1 \\ h = 1 \end{cases}$; the problem to solve is: AX = B.

The tests were run on an IBM.

4.5.1. Decomposition 4B + I. As the nodes are numbered domain by domain, the new ordering is: 1,3,6/10,12,15/2,5,7/11,14,16/ 8,9,4,13.

Suppose $D = \frac{100}{6}$; the solution of AX = B, with:

$B = {}^t(0, 0,-202, 0, 0,-202, 0, 0,-202, 0, 0,-202,0,0,0,0)$

$X = {}^t(100,100, 2,100,100, 2,100,100, 2,100,100, 2,0,0,0,0)$.

We take $X^{(0)} = X$ and perform 50 iterations. We should have $X^{(n)} \approx X$ (numerically) at each iteration ; but after a certain number of iterations, $X^{(n)}$ becomes different from X, and the error increases (see fig. 10).

This phenomenon doesn't appear in the two other cases.

In the case $D = \frac{1}{6}$, we wanted to see the influence of a slight modification of the initial vector. We took:

$B = {}^t(0,0,-4,0,0,-4,0,0,-4,0,0,-4,0,0,0,0)$ so that:

$X = {}^t(1,1, 2,-1,1,2,1,-1,2,-1,-1,2,0,0,0,0)$; we choose:

$X^{(0)} = {}^t(0,0,8,0,0,8,0,0,8,0,0,8,0,0,0,0)$ to have a convergence in one iteration, and $X_\varepsilon^{(0)} = (0,0,8,0,0,8,0,0,8,0,0,8,\varepsilon,\varepsilon,\varepsilon,\varepsilon)$ with $\varepsilon = 0{,}1$. During the first iterations, the results are different ; the error reduces, but at least during the ten first iterations, $|X^{(n)}(i) - X_\varepsilon^{(n)}| > 10^{-4}$ $\forall i$.

4.5.2. Decomposition 4B. The phenomenon described above doesn't appear. We note that the performance deteriorate as D increases. In the case $D = \frac{100}{6}$, the best approximation of 0 on the interface

ITERATION	1	error
I= 1	X(I)= 99.9999390	ε
I= 2	X(I)= 99.9999390	ε
I= 3	X(I)= 2.00000000	0
I= 4	X(I)= -99.9999390	ε
I= 5	X(I)= 99.9999390	ε
I= 6	X(I)= 2.00000000	0
I= 7	X(I)= 99.9999390	ε
I= 8	X(I)= -99.9999390	ε
I= 9	X(I)= 2.00000000	0
I= 10	X(I)= -99.9999390	ε
I= 11	X(I)= -99.9999390	ε
I= 12	X(I)= 2.00000000	0
I= 13	X(I)= 0.000000000E+00	0
I= 14	X(I)= 0.000000000E+00	0
I= 15	X(I)= 0.000000000E+00	0
I= 16	X(I)= 0.000000000E+00	0

ITERATION	2
I= 1	X(I)= 99.9999390
I= 2	X(I)= 99.9999390
I= 3	X(I)= 2.00000000
I= 4	X(I)= -99.9999390
I= 5	X(I)= 99.9999390
I= 6	X(I)= 2.00000000
I= 7	X(I)= 99.9999390
I= 8	X(I)= -99.9999390
I= 9	X(I)= 2.00000000
I= 10	X(I)= -99.9999390
I= 11	X(I)= -99.9999390
I= 12	X(I)= 2.00000000
I= 13	X(I)= 0.238418434E-04
I= 14	X(I)= 0.238418434E-04
I= 15	X(I)= 0.238418434E-04
I= 16	X(I)= 0.238418434E-04

ITERATION	3
I= 1	X(I)= 99.9999695
I= 2	X(I)= 99.9999695
I= 3	X(I)= 2.00000095
I= 4	X(I)= -99.9999390
I= 5	X(I)= 99.9999237
I= 6	X(I)= 2.00000000
I= 7	X(I)= 99.9999237
I= 8	X(I)= -99.9999390
I= 9	X(I)= 2.00000000
I= 10	X(I)= -99.9999390
I= 11	X(I)= -99.9999390
I= 12	X(I)= 2.00000000
I= 13	X(I)= 0.238418434E-04
I= 14	X(I)= 0.238418434E-04
I= 15	X(I)= 0.238418434E-04
I= 16	X(I)= 0.238418434E-04

ITERATION	10
I= 1	X(I)= 99.9998627
I= 2	X(I)= 99.9998627
I= 3	X(I)= 1.99999809
I= 4	X(I)= -99.9999847
I= 5	X(I)= 99.9999847
I= 6	X(I)= 2.00000191
I= 7	X(I)= 99.9999847
I= 8	X(I)= -99.9999847
I= 9	X(I)= 2.00000191
I= 10	X(I)= -99.9998627
I= 11	X(I)= -99.9998627
I= 12	X(I)= 1.99999809
I= 13	X(I)= 0.119209217E-03
I= 14	X(I)=-0.953673734E-04
I= 15	X(I)= 0.119209217E-03
I= 16	X(I)=-0.953673734E-04

ITERATION	20
I= 1	X(I)= 100.001541
I= 2	X(I)= 100.001541
I= 3	X(I)= 2.00004864
I= 4	X(I)= -99.9983063
I= 5	X(I)= 99.9983063
I= 6	X(I)= 1.99995136
I= 7	X(I)= 99.9983063
I= 8	X(I)= -99.9983063
I= 9	X(I)= 1.99995136
I= 10	X(I)= -100.001541
I= 11	X(I)= -100.001541
I= 12	X(I)= 2.00004864
I= 13	X(I)=-0.321864872E-02
I= 14	X(I)= 0.324249058E-02
I= 15	X(I)=-0.321864872E-02
I= 16	X(I)= 0.324249058E-02

ITERATION	30
I= 1	X(I)= 99.9513550
I= 2	X(I)= 99.9513550
I= 3	X(I)= 1.99853516
I= 4	X(I)= -100.048492
I= 5	X(I)= 100.048492
I= 6	X(I)= 2.00146484
I= 7	X(I)= 100.048492
I= 8	X(I)= -100.048492
I= 9	X(I)= 2.00146484
I= 10	X(I)= -99.9513550
I= 11	X(I)= -99.9513550
I= 12	X(I)= 1.99853516
I= 13	X(I)= 0.975369811E-01
I= 14	X(I)=-0.975131392E-01
I= 15	X(I)= 0.975369811E-01
I= 16	X(I)=-0.975131392E-01

ITERATION	40
I= 1	X(I)= 101.469406
I= 2	X(I)= 101.469406
I= 3	X(I)= 2.04430580
I= 4	X(I)= -98.5304413
I= 5	X(I)= 98.5304413
I= 6	X(I)= 1.95569420
I= 7	X(I)= 98.5304413
I= 8	X(I)= -98.5304413
I= 9	X(I)= 1.95569420
I= 10	X(I)= -101.469406
I= 11	X(I)= -101.469406
I= 12	X(I)= 2.04430580
I= 13	X(I)= -2.94999886
I= 14	X(I)= 2.95002270
I= 15	X(I)= -2.94999886
I= 16	X(I)= 2.95002270

ITERATION	50
I= 1	X(I)= 55.5384216
I= 2	X(I)= 55.5384216
I= 3	X(I)= 0.659451008
I= 4	X(I)= -144.461411
I= 5	X(I)= 144.461395
I= 6	X(I)= 3.34054852
I= 7	X(I)= 144.461395
I= 8	X(I)= -144.461411
I= 9	X(I)= 3.34054852
I= 10	X(I)= -55.5383911
I= 11	X(I)= -55.5383911
I= 12	X(I)= 0.659450054
I= 13	X(I)= 89.2581329
I= 14	X(I)= -89.2581329
I= 15	X(I)= 89.2581329
I= 16	X(I)= -89.2581329

FIG.10: *Decomposition 4B + I*. $D = \frac{100}{6}$, $X^{(0)} = X$.

seems to be of the order of 2.10^{-5}.

4.5.3. **Decomposition 2B + I.** The new ordering of the nodes is: 1,2,3,4,5,6,7/10,11,12,13,14,15,16/8,9. We choose $D = \frac{100}{6}$. For
$B = {}^t(0,0,0,0,0,-202,-202,0,0,0,0,0,-202,-202,0,0)$,
$X = {}^t(100,100,100,0,-100,2,2,-100,-100,100,0,-100,2,2,0,0)$. If we take $X^{(0)} = {}^t(0,0,0,0,0,100,100,0,0,0,0,0,100,100,0,0)$, the block Jacobi method converges theoretically in one iteration. Then take
$X_\varepsilon^{(0)} = {}^t(0,0,0,\varepsilon,0,100,100,0,0,0,\varepsilon,0,100,100,0,0)$ and $\varepsilon = 0,1$. Even with $X^{(0)}$, the approximation is not better than 10^{-4} ; with $X_\varepsilon^{(0)}$ we have (almost) the same results.

The phenomenon described for decomposition 4B + I doesn't seem to occur.

4.5.4. **Some observations.** A modification of $X^{(0)}(i)$, i corresponding to a node representing the gradient on an axis of symmetry, has more influence if the node is on the axis of decomposition. The results indicates that decomposition 4B + I is less stable than decomposition 4B, and also than 2B + I.

5. **Conclusion.** When everything is symmetrical, the Jacobi method can converge in one iteration with a decomposition of dissection type, if an appropriate initial vector is choosen.

The decompositions in which the interface is separated give faster results when a not too high precision is requested ; but they cannot reach a very high precision, and in this case the results may deteriorate. This can be partly explained by the fact that after some outer iterations, the initialization vector of the Jacobi iterations has no more exactly the properties for a convergence in one iteration.

Decompositions for which the interface is separated seem to be less stable than the ones in which the interface is integrated to the domains.

The choice of the decomposition depends on what we need: a high precision or a fast result.

REFERENCES

(1) J.M. COLLART, C. FEDON-MAGNAUD, J.J. LAUTARD, Parallel Diffusion Calculation for the Phaeton on-line Multiprocessor Computer, Proceedings of the International Topical Meeting on Advances in Reactor Physics, Mathematics and Computation, Paris April 27-30, 1987.
(2) J.M. COLLART, C. FEDON-MAGNAUD, J.J. LAUTARD, The Phaeton Project, ENC 86 Transactions, 2, p 303, Geneva, June 1-6, 1986.
(3) F. COULOMB, C. FEDON-MAGNAUD, Mixed and Mixed Hybrid Elements for the Diffusion Equation, Proceedings of the International Topical Meeting on Advances in Reactor Physics, Mathematics and Computation, Paris April 27-30, 1987.
(4) R. DAUTRAY, J.L. LIONS, Analyse mathématique et calcul numérique pour les sciences et techniques, R. Dautray, Masson, 1985.
(5) J.J. DUDERSTADT, L.J. HAMILTON, Nuclear Reactor Analysis, J. Wiley & Sons, Inc.
(6) P.A. RAVIART, J.M. THOMAS, A Mixed Finite Element Method for 2nd Order Elliptic Problems, Mathematical Aspects of the Finite Element Method, Lecture Notes in Mathematics 606 Springer Verlag, 1977.
(7) J.M. THOMAS, Sur l'analyse numérique des méthodes d'éléments finis hybrides et mixtes, Thesis, Université P. et M. Curie, 1977.